

A Viroimmunologic Model to Characterize the Antiviral Effect of Molnupiravir in Outpatients Infected With SARS-CoV-2: Implication for Treatment Duration

Bach Tran Nguyen,^{1,©} Julie Bertrand,^{1,©} Akosua A. Agyeman,² Shengyuan Zhang,² Ly-Mee Yu,^{3,©} Victoria Harris,^{3,©} Paul Little,^{4,©} Christopher C. Butler,^{3,©} Judith Breuer,^{2,©} David M. Lowe,^{5,6,©} Joseph F. Standing,^{2,7,©} and Jérémie Guedj^{1,a,©}; on behalf of the PANORAMIC study group^b

¹Université Paris Cité and Université Sorbonne Paris Nord, Inserm, IAME, France; ²Infection, Immunity and Inflammation, Great Ormond Street Institute of Child Health, University College London; ³Nuffield Department of Primary Care Health Sciences, University of Oxford; ⁴Primary Care Research Centre, University of Southampton; ⁵Institute for Immunity and Transplantation, University College London; ⁶Department of Clinical Immunology, Royal Free London NHS Foundation Trust; and ⁷Department of Pharmacy, Great Ormond Street Hospital for Children NHS Trust, London, United Kingdom

Background. The antiviral efficacy of molnupiravir against SARS-CoV-2 is controversial. Here, we develop a model integrating viral and immune dynamics to characterize the mechanism of action of molnupiravir in vivo and its impact on viral dynamics during and after treatment.

Methods. We analyzed data from the PANORAMIC trial, where 577 outpatients were randomized shortly after symptom onset to receive usual care or molnupiravir for 5 days, with viral and immunologic data collected within 2 weeks. We developed a mathematical model that characterized virus-host interaction, accounting for the impact of molnupiravir on viral replication and mutagenesis. The model was used to explore the impact of longer treatment duration.

Results. Molnupiravir reduced RNA replication with an efficacy that reached 93% at the end of a 5-day treatment. This effect was mediated through 2 pathways: 1 that increased transition mutation frequency and 1 that directly inhibited viral production. Accordingly, 5-day treatment shortened the median time to clearance of RNA and infectious virus by approximately 2 days. Ten-day treatment could reduce the time to RNA clearance by 5 days and the occurrence of viral rebounds. Longer treatment durations might be needed for postexposure prophylaxis.

Conclusions. Our model suggests that molnupiravir acts primarily on viral replication, and not specifically on viral infectivity. Longer administration of molnupiravir may reduce the rebound rate, shortening the time to viral clearance.

Keywords. molnupiravir; mutagenesis; SARS-CoV-2; treatment duration; viral clearance.

Despite its protection against severe SARS-CoV-2 infection, vaccination is less effective in high-risk populations, including individuals who are immunocompromised and those who are elderly [1]. Thus, it remains critical to develop effective treatments that prevent disease progression and onward transmission. Among candidate agents, molnupiravir is authorized for

emergency use by the US Food and Drug Administration in some high-risk populations. However, clinical trials for molnupiravir showed low benefits. While molnupiravir may shorten times to symptom resolution [2] and reduce the occurrence of post–COVID-19 symptoms [3, 4], its impact on severe disease is probably marginal, at least in vaccinated populations [3].

Regarding virologic efficacy, molnupiravir likely increases the rate of viral clearance [2, 5, 6]. In some studies, molnupiravir was associated with increased rates of detectable virus after treatment completion [7], posing the question of adequate treatment duration. Furthermore, a signature of molnupiravirinduced mutations was found in populations where molnupiravir was used, suggesting that some highly mutated viruses could be viable and capable of onward transmission [8]. These conflicting results have resulted in the drug's withdrawal by several regulatory agencies, including the European Medicines Agency [9]. Because antiviral effect is a prerequisite to clinical efficacy [10] and drugs with a similar mechanism of action could be developed in the future, it remains important to understand how molnupiravir affects viral dynamics.

Here, we address this question by developing a modeling framework to characterize the virologic, immunologic, and

The Journal of Infectious Diseases® 2025;231:e1080–90

© The Author(s) 2025. Published by Oxford University Press on behalf of Infectious Diseases Society of America.

This is an Open Access article distributed under the terms of the Creative Commons Attribution-NonCommercial-NoDerivs licence (https://creativecommons.org/licenses/by-nc-nd/4.0/), which permits non-commercial reproduction and distribution of the work, in any medium, provided the original work is not altered or transformed in any way, and that the work is properly cited. For commercial re-use, please contact reprints@oup.com for reprints and translation rights for reprints. All other permissions can be obtained through our RightsLink service via the Permissions link on the article page on our site—for further information please contact journals.permissions@oup.com.

https://doi.org/10.1093/infdis/jiaf158

Received 17 October 2024; editorial decision 21 March 2025; accepted 21 March 2025; published online 1 April 2025

^aJ. F. S. and J. G. share joint senior authorship.

^bStudy team members are listed in the acknowledgments.

Correspondence: Bach Tran Nguyen, PhD, Université Paris Cité and Université Sorbonne Paris Nord, INSERM, IAME, 16 rue Henri Huchard, Paris cedex 18 75870, France (tran-bach. nguyen@inserm.fr). Jérémie Guedj, PhD, Université Paris Cité and Université Sorbonne Paris Nord, INSERM, IAME, 16 rue Henri Huchard, Paris cedex 18 75870, France (jeremie.guedj@inserm.fr)

mutation data observed in the PANORAMIC trial, one of the most detailed studies evaluating molnupiravir efficacy. Using this model, we discuss molnupiravir's antiviral effect and adequate treatment duration.

METHODS

Study Design and Population

The study population was previously presented in detail [7]. In brief, from December 2021 to April 2022, the PANORAMIC study included eligible participants of both sexes aged ≥50 or >18 years with relevant comorbidities. Participants were randomly assigned to receive usual care alone or with 800 mg of oral molnupiravir twice daily for 5 days.

Ethical Approval

The PANORAMIC study (ISRCTN30448031) was approved by the UK Medicines and Healthcare products Regulatory Agency and the South Central–Berkshire Research Ethics Committee of the Health Research Authority (ethics approval reference 21/SC/0393).

Sample Collection

Overall 577 participants were enrolled [2, 7] and provided self-collected nasopharyngeal swabs. All participants returned dried blood spot samples collected on days 1, 5, and 14 (Figure 1). All samples were taken by participants and returned to a central laboratory by post.

Analytic Methods

The analytic methods were previously described for virology, immunology, mutation, and culture data [7]. In brief, viral load had a lower limit of quantification of 109 copies/mL; mutations were quantified by sequencing samples positive for SARS-CoV-2. Sequencing was performed for a target depth of 5000× per genome on an Illumina sequencer with $2 \times \ge 75$ -base pair paired-end reads, with positive and negative controls included to detect contamination at each step. For viral culture, samples were aliquoted into a tube containing Bovine Albumin Fraction V (7.5%), stored at 4 °C, and then moved to storage at -80 °C within 24 hours. Spike antibodies were measured by immunoassay (Elecsys Anti-SARS-CoV-2 S; Roche) with a validated 10-fold dilution factor correction applied.

Modeling Viral Load and Spike Antibodies in Untreated Patients

First, we characterized viral and immune kinetics in untreated patients—specifically, those receiving usual care alone. Three models were tested: a target-cell limited model, a refractory model, and a cytotoxic model [11]. The target-cell limited model includes 3 types of cell populations: target cells susceptible to infection (T), infected cells in an eclipse phase (I_I) , and infected cells actively producing virus (I_2) . Susceptible target cells are infected at an infection rate β (mL/virion/d). After a mean eclipse

phase of $1/\kappa$ days, infected cells (I_I) become productive (I_2) , producing virions at rate π and are lost at a per capita rate δ . The virions generated can be infectious (V_I) in proportion μ , while the remaining proportion $(1-\mu)$ is noninfectious (V_{NI}) . The total viral load is the sum of V_I and V_{NI} , both cleared at the same rate c. In the refractory model, susceptible target cells become refractory at rate ϕ_R , and refractory cells revert to a susceptible state at rate ρ . In the cytotoxic model, we investigated the effect on the loss rate of infected cells $\delta = \delta_0 \times \left(1 + \frac{\phi_\delta I_2}{I_2 + I_{50}}\right)$, where δ_0 represents their initial value and $\phi_\delta \times I_2/(I_2 + I_{50})$ indicates the increase under the cytotoxic effect depending on the number of productive infected cells. The 3 models can be written as follows (with ϕ_R and ρ at 0 in the target-cell limited version):

$$dT/dt = -\beta V_I T - \phi_R I_2 T + \rho R$$

$$dR/dt = \phi_R I_2 T - \rho R$$

$$dI_1/dt = \beta V_I T - \kappa I_1$$

$$dI_2/dt = \kappa I_1 - \delta I_2$$

$$dV_I/dt = \pi I_2 - cV_I$$

$$dV_{NI}/dt = (1-\pi)I_2 - cV_{NI}$$

Spike antibody kinetics was described via a Gompertz function: $A(t) = A_{max} \times e^{-e^{\alpha_1 - \alpha_2(t + t_I - t_A)}}$, where A_{max} represents the maximum antibody level, α_1 and α_2 correspond to the asymptote coefficient and inherent production rate, t_I is the delay between symptom onset and infection, and t_A is the time of inflexion in days from infection. We used an E_{max} -type function to characterize the antibody effect: $E_A(t) = \varepsilon_A \times A(t)/(A(t) + A_{50})$, with A_{50} equating to spike antibodies producing 50% of the maximal effect and ϵ_A indicating the maximal antibody effect on viral load. We investigated different models for antibody effect, either on viral infectivity, $\beta(t) = \beta_0 \times (1 - E_A(t))$, or the loss rate of infected cells, $\delta(t) = \delta_0 \times (1 + E_A(t))$.

Modeling Viral Load, Spike Antibodies, and Mutation Proportion Under a Molnupiravir Effect

Molnupiravir Antiviral Effect on Viral Load

In the absence of measured pharmacokinetics, we used a phenomenologic model [12] to describe how molnupiravir drug efficacy, noted $E_{M\to V}(t)$, changes over time (Supplementary Text 1):

$$\begin{split} E_{M \to V}(t) \\ &= \begin{cases} \frac{\varepsilon_{M \to V} \times (1 - e^{-k(t - t_{start})})}{1 - \varepsilon_{M \to V} \times e^{-k(t - t_{start})}}, \ t_{start} \leq t \leq t_{end} \\ \frac{\varepsilon_{M \to V} \times (1 - e^{-k(t_{end} - t_{start})})}{\varepsilon_{M \to V} \times (1 - e^{-k(t_{end} - t_{start})}) + (1 - \varepsilon_{M \to V}) \times e^{k(t - t_{end})}}, \ t > t_{end} \end{cases} \end{split}$$

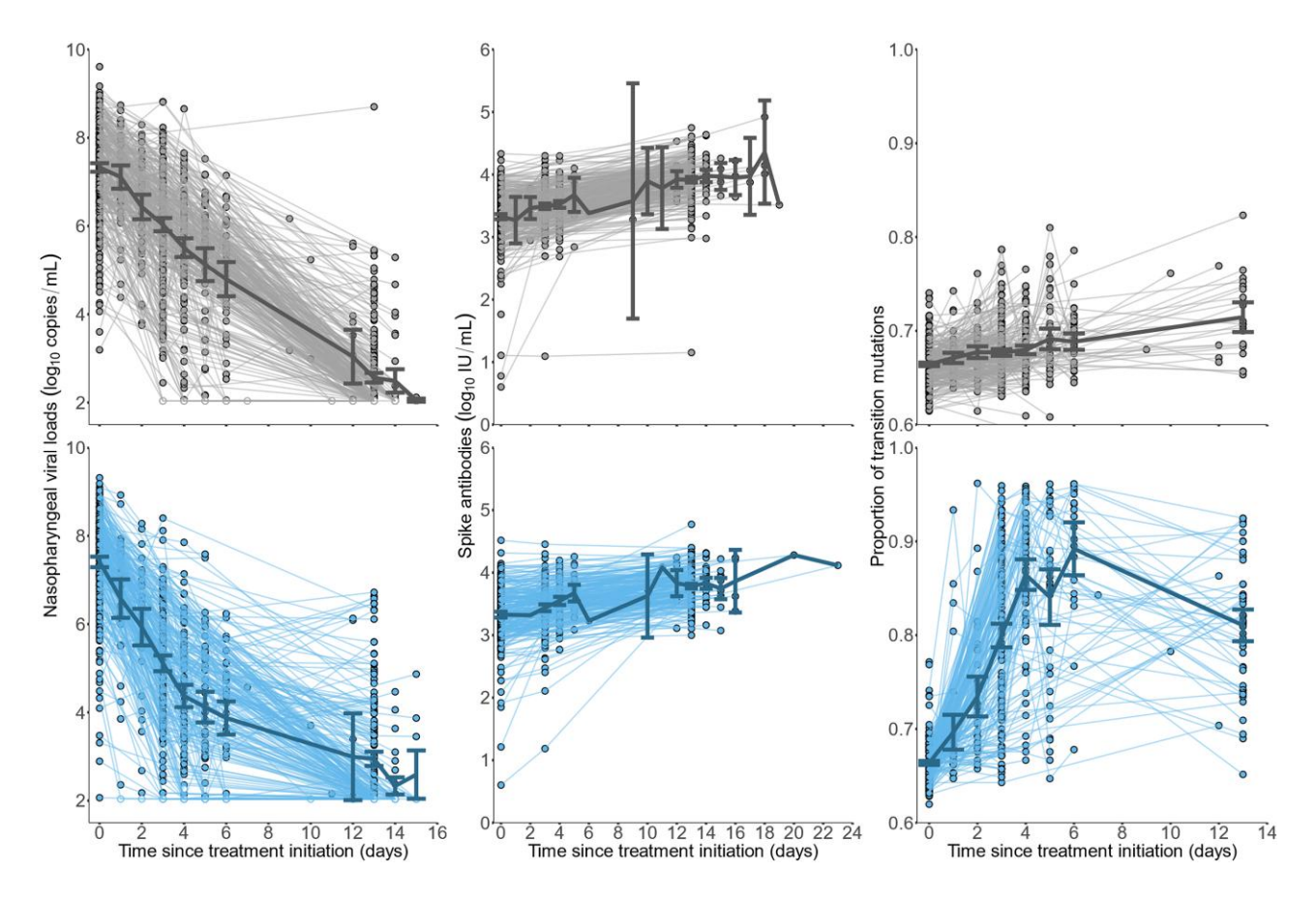


Figure 1. Nasopharyngeal viral load (left), spike antibodies (middle), and proportion of transition mutations (right) in the PANORAMIC trial. Upper, usual care alone (untreated, n = 324); lower, usual care with molnupiravir, 800 mg, twice a day (treated, n = 253); circles, observed data; empty circles, data below the limit of quantification; bold solid lines, mean; bold whiskers, 90% CI.

where $\varepsilon_{M \to V}$ is the molnupiravir maximal efficacy at drug steady state and k is the rate of drug (intracellular) elimination.

We then used the model to fit data from untreated and treated participants. We explored 2 models for a molnupiravir effect of reducing either the proportion of infectious virus, $\mu(t) = \mu_0 \times (1 - E_{M \to V}(t))$, or the rate of viral production per infected cell, $\pi(t) = \pi_0 \times (1 - E_{M \to V}(t))$. We also compared this with a model of constant drug efficacy that does not change over time.

Transition Mutation Impact on Viral Kinetics and the Effect of Molnupiravir

Next, we characterized how molnupiravir acts on virus mutagenesis, noting $E_{M\to P}$ as the effect of molnupiravir in increasing the transition mutation rate, P(t):

$$log\left(\frac{P(t)}{1-P(t)}\right) = log\left(\frac{P_0}{1-P_0}\right) + k_P \times t + E_{M \to P}(t),$$

where P_0 and k_P denote, respectively, the initial value at infection time and the natural rate of increase in transition mutations over time without molnupiravir. We assumed a linear effect of molnupiravir on the logit scale as

 $E_{M\to P}(t) = \varepsilon_{M\to P} \times C(t)$, with C(t) being the drug concentrations (Supplementary Text 1). As the effect could be delayed after molnupiravir initiation (Figure 2), we also tested an effect compartment model, where $E_{M\to P}(t) = \varepsilon_{M\to P} \times C_e(t)$, with $C_e(t)$ being the drug concentrations in the effect compartment, given by $dC_e/dt = k_{e0} \times (C(t) - C_e(t))$.

We then determined the impact of these transition mutations on viral kinetic parameters with an efficacy, noted ε_P , in reducing either the proportion of infectious virus, $log\left(\frac{\mu(t)}{1-\mu(t)}\right) = log\left(\frac{\mu_0}{1-\mu_0}\right) - \varepsilon_P \times [k_P \times t + E_{M \to P}(t)]$, or the rate of viral production per infected cell, $log(\pi(t)) = log(\pi_0) - \varepsilon_P \times [k_P \times t + E_{M \to P}(t)]$.

Impact on the Rate of Positive Viral Culture

Finally, using a logistic model, we tested whether the probability of positive culture was associated with the amount of infectious virus, $V_I(t)$, and/or treatment intake.

Assumption on Parameter Values

Several parameters of the viral kinetic model were fixed to ensure identifiability [13, 14]. Infection time was fixed to 3 days

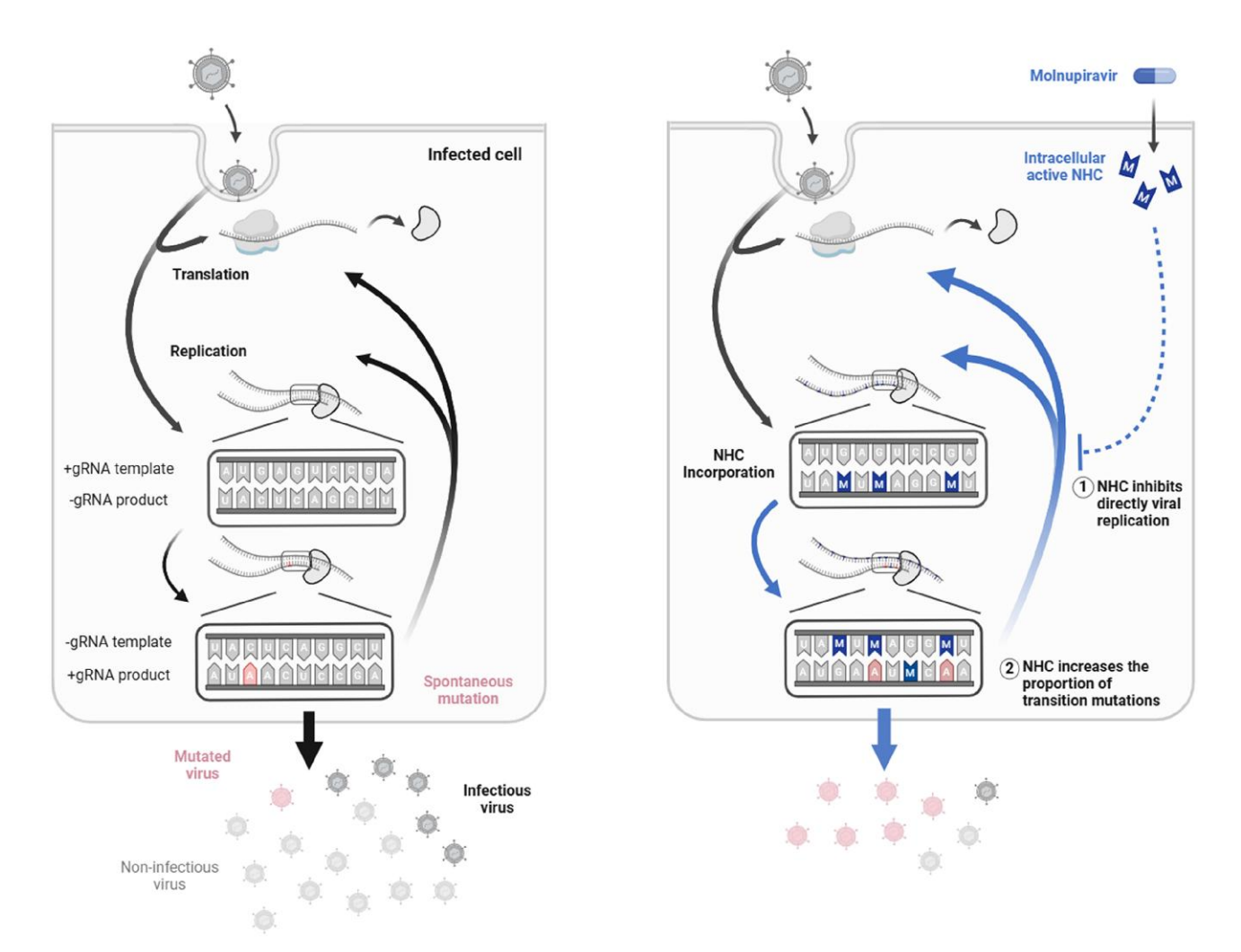


Figure 2. Model for molnupiravir effect on SARS-CoV-2 replication. Abbreviation: NHC, N4-hydroxycytidine. Created in BioRender. Guedj, J. (2025) https://BioRender.com/k72z109

before symptom onset [15, 16]. Since only the product $\pi_0 \times T_0$ is identifiable, we fixed the initial density of target cells, T_0 , to 4×10^6 cells/mL for a typical volume of 30 mL [14]. The viral clearance rate, c, was set to 10 days⁻¹, κ was fixed to 4 days⁻¹ (representing a mean eclipse phase of 6 hours), and the initial proportion of infectious virus μ_0 was fixed to 10^{-4} . For molnupiravir pharmacokinetics, the constant k was set to 2.5 days⁻¹, corresponding to a 6-hour intracellular half-life [17].

Model-Building Strategy

A nonlinear mixed effect model was used to determine the viroimmunologic model, first in untreated participants. Then, a model including the molnupiravir effect was fitted to treated and untreated individuals. All estimations were performed by the stochastic approximation expectation-maximization algorithm implemented in Monolix (Monolix Suite 2021R2). Random effects with an SD <0.1 or associated with a relative standard error >100% were removed via a backward procedure and kept only if, following their removal, the corrected bayesian

information criterion increased by >2 points. Goodness of fit was assessed by visually inspecting individual fit and residual scatter plots.

Covariates were explored only in the final model and were limited to those with <10% of missing data and >10% of prevalence [2, 7]. Next, correlations between covariates and individual parameter estimates were preselected with a threshold at $P \le .05$. Final covariate selection was performed by the COSSAC algorithm [18].

Model Predictions Following Different Treatment Courses

To assess the therapeutic efficacy of treatment durations, we simulated 100 replicates of 250 individuals (approximating the number of treated individuals in PANORAMIC) using estimates from the final model and different durations of treatment, with time of treatment initiation sampled from the distribution observed in PANORAMIC. We also examined the impact of postexposure prophylaxis, assuming that treatment was given 1 day postinfection in all individuals [7]. We

calculated the following metrics for each individual: viral load on day 5 posttreatment, time to first negative result on polymerase chain reaction (PCR; viral load below limit of quantification), occurrence of viral rebound (defined as 1 viral load ≥ 3 log₁₀ copies/mL within 14 days after treatment completion, with an increase $\geq 1.0 \log_{10} \text{ copies/mL}$ vs treatment completion), and the area under the curve of transition mutation load ($[V_I(t) + V_{NI}(t)] \times P(t)$) over time from treatment initiation to sustained negative PCR result. Regarding viral culture, we calculated for each simulated individual the probability of developing a positive result and then the time to achieve <5% of positive culture. To evaluate the risk of repositive culture after treatment completion, we sampled from the probability distribution to calculate the proportion of positive individuals, assuming daily sampling in the 14 days after treatment completion. Next, we calculated the median value over all individuals in each replicate and then provided the median and its 90% confidence interval (90% CI) over 100 replicates. We also performed a sensitivity analysis, assuming that molnupiravir directly affects virus infectivity.

RESULTS

SARS-CoV-2 Viral Kinetics in the Absence of Molnupiravir

A model including an infection-refractory compartment best described observed viral load (Figure 3, Table 1, Supplementary Table 1). The death rate of productive infected cells, δ_0 , was estimated at 0.64 day⁻¹, equivalent to a 25-hour half-life, with a production rate of 4.8×10^4 virions.cell⁻¹.day⁻¹. Peak viral load was estimated at 8.2 log₁₀ copies/mL (90% CI, 8.2-8.3) and coincided with symptom onset (median delay between viral peak and symptom onset, 0 days; 90% CI, 0-1). Spike antibodies increased rapidly after inclusion and reached 90% of their maximal effect (noted A_{90}) 18 days after symptom onset (90% CI, 18–19), with a level of 1.7×10^4 IU/mL (90% CI, $7.4 \times 10^3 - 2.6 \times 10^4$). In this model, spike antibodies at their maximal effect increased the elimination of infected cells by approximatively 100%, therefore reducing their half-life by 50%. Overall, the median time to first undetectable RNA, called "viral clearance" in the following, was estimated at 13.5 days after symptom onset (90% CI, 13.5-14.5). This time would be extended to 2.0 days longer (90% CI, 1.0-3.0) in males than females due to a lower antibody increase rate (Supplementary Figure 1).

Molnupiravir Increases Transition Mutations and Strongly Inhibits Viral Replication

A model assuming that molnupiravir reduces viral production rate, $\pi(t)$, best described viral load data (Figure 2):

$$dV_I/dt = \pi(t)I_2 - cV_I$$

$$dV_{NI}/dt = (1-\pi(t))I_2-cV_{NI},$$

where
$$\pi(t) = \pi_0 * (1 - E_{M \to V}(t)) * e^{-\varepsilon_P \times [k_P \times t + E_{M \to P}(t)]}$$
.

The maximal direct effect of molnupiravir in inhibiting viral production, $\epsilon_{M\to V}$, was estimated at 67% (90% CI, 66%–68%; Table 1, Supplementary Table 2). Considering molnupiravir's effect on mutations, our model predicted that molnupiravir strongly increased the rate of transition mutations from 66% (90% CI, 66%-66%) at treatment initiation to 88% (90% CI, 87%-89%) on day 5 (Figure 4). This effect on transition mutation inhibited the viral replication rate by 76% (90% CI, 70%-80%; Figure 5). Thus, molnupiravir inhibited viral replication via mutation-independent $(E_{M \to V})$ and mutation-mediated $(E_{M\rightarrow P})$ mechanisms (Supplementary Tables 3 and 4). Together, these effects led to a strong inhibition of viral replication, estimated to 93% (90% CI, 92%-94%) at treatment completion. The action on transition mutation rate was also more sustained, maintaining a high viral inhibition, >70% up to 2.0 days (90% CI, 2.0-3.0) after treatment completion. Consequently, 5-day molnupiravir shortened the time to viral clearance by 1.5 days (90% CI, 0.5-2.5) as compared with untreated individuals.

Molnupiravir Shortens the Clearance of Infectious Virus

A model assuming an association between positive culture and the amount of infectious virus, V_I , best described the data (odds ratio, 4.68; 90% CI, 3.71–5.65; Supplementary Figure 2, Supplementary Table 5). The model predicted that molnupiravir lowered the amount of infectious virus via an inhibition of viral RNA, decreasing the time to clearance of infectious virus, with a median time to achieve 5% viral culture positivity of 2.5 days (90% CI, 2.5–3.0) vs 5.0 days (90% CI, 4.5–5.5) in untreated individuals (Figure 6). Incorporating an independent effect of molnupiravir intake did not improve model predictions.

Impact of Different Treatment Durations

Next we evaluated how different treatment durations affect viral kinetics (Figure 4). Although a 5-day regimen would reduce the median times to clearance for viral RNA and infectious virus by approximately 2 days, the model predicted that viral load remained detectable in the majority of patients (82%) at treatment completion. Consequently, treatment interruption could also increase the rate of viral rebound to 5% (90% CI, 3%–8%) vs 0% (90% CI, 0–.4%) in untreated individuals. Longer treatment could decrease the time to undetectable PCR to 12, 11, 9, and 9 days following 5-, 7-, 10-, and 14-day regimens, respectively. Accordingly, viral rebound rates would decrease with longer treatment duration, with predicted value of 5%, 5%, 4%, and 3% following 5-, 7-, 10-, and 14-day regimens. Notably, longer treatment would have only a minimal effect on time to clearance of infectious virus (Figure 6).

We conducted similar simulations assuming that molnupiravir would be given, not as a curative treatment as done in PANORAMIC trial, but as a postexposure prophylaxis given 1 day after infection. A treatment duration <10 days increased

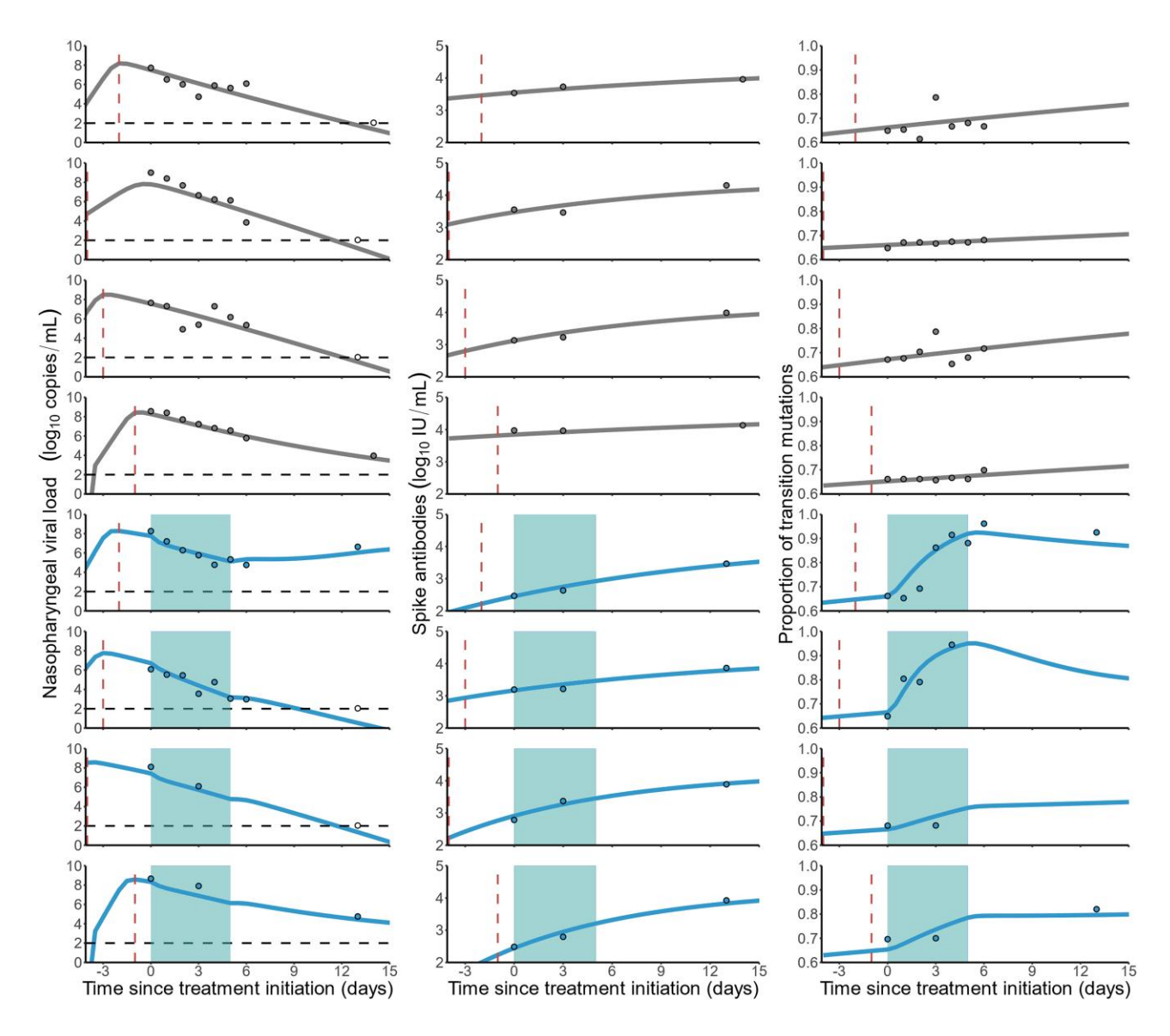


Figure 3. Individual fits for nasopharyngeal viral load (left), spike antibodies (middle), and proportion of transition mutation (right) from 8 PANORAMIC participants. Gray circles, observed data; white circles, data below the limit of quantification; solid curves, model predictions (gray, untreated; blue, treated); black horizontal dashed lines, limit of quantification; red vertical dashed lines, symptom onset; shaded area, molnupiravir treatment period.

the time to viral clearance and virologic burden as compared with untreated individuals (Supplementary Figures 3 and 4).

Finally, we verified that a model assuming that molnupiravir acts directly on viral infectivity (ie, decreases the proportion of infectious virus, noted μ ; Supplementary Table 6) would provide similar conclusions on the optimal treatment duration (Supplementary Figure 5).

DISCUSSION

In this article, we developed a mathematical model to fit virologic, immunologic, and mutagenesis data in patients treated with molnupiravir. Our findings suggest that molnupiravir was largely effective, inhibiting viral replication by 93% at the end

of 5-day regimens. While 5-day molnupiravir shortened the median time to viral clearance by about 2 days, our model predicted that 10-day regimens could further shorten time to viral clearance and reduce viral rebound rates after treatment completion.

Mechanistically, our model assumes that molnupiravir inhibits viral replication [19], with a mechanism that directly affects viral production and another one mediated by an increased transition mutation rate. This mechanism of action can be explained by 2-step viral inhibition [20, 21], characterized by relatively high selectivity of molnupiravir for incorporation as a cytidine triphosphate analogue, followed by indiscriminate incorporation of either triphosphorylated adenosine (mutagenesis) or guanosine with molnupiravir localized in the template. This distinguishes molnupiravir from

Table 1. Final Estimates for Data on Nasopharyngeal Viral Load, Spike Antibodies, and Proportion of Transition Mutation in PANORAMIC Trial

Parameter (Unit)		Estimate (RSE, %)	IIV (RSE, %)
Viral kinetics			
Viral infectivity (copy ⁻¹ .mL.d ⁻¹)	β	1.2×10^{-5} (14)	
Conversion rate from target cells to refractory cells (cell ⁻¹ .d ⁻¹)	ϕ	3.2×10^{-5} (142)	3.17 (7)
Conversion rate from refractory cells to target cells (d ⁻¹)	ρ	2.2×10^{-3} (40)	1.79 (17)
Initial loss rate of infected cells (d ⁻¹)	$\delta_{\it O}$	0.64 (5)	
Initial number of virions produced from infected cells (copies.cells ⁻¹ .mL ⁻¹ .d ⁻¹)	π_{O}	4.8×10^4 (30)	0.57 (38)
Maximal effect size of molnupiravir on viral production	$\epsilon_{\mathcal{M} o V}$	0.67 (9)	1.07 (33)
Spike antibodies			
Maximum spike antibodies (IU.mL ⁻¹)	A_{max}	2.4×10^4 (8)	0.5 (6)
Asymptote coefficient	α_1	0.56 (9)	0.33 (11)
Inherent production rate	α_2	0.05 (6)	0.60 (6)
Time of inflexion from infection (days)	$t_{\mathcal{A}}$	9.31 (5)	
Maximal antibody effect on infected cell elimination	$\epsilon_{\mathcal{A}}$	1.08 (14)	0.72 (6)
Spike antibodies producing 90% maximal effect (IU.mL ⁻¹)	A ₉₀	1.7×10^4 (33)	
Viral mutation			
Initial proportion of transition mutations	P_{0}	0.65 (0.3)	
Growth rate of transition mutation proportion (d ⁻¹)	k _P	0.02 (8)	0.01 (12)
Transfer rate between molnupiravir plasma and effect compartments (d ⁻¹)	k _{e0}	0.50 (45)	0.85 (9)
Effect size of molnupiravir on transition mutation proportion	$\epsilon_{M o P}$	3.09 (9)	0.37 (21)
Effect size of transition mutation proportion on viral production	ϵ_P	1.09 (15)	0.61 (19)
Covariates			
Effect size of age on transfer rate from target cells to refractory cells (ln.y ⁻¹)	$eta_{Age/\phi}$	-0.07 (39)	
Effect size of age on transfer rate between molnupiravir pharmacokinetic compartments (ln.y ⁻¹)	$eta_{Age/ke0}$	-0.03 (29)	
Effect size of male on antibody asymptote coefficient	β _{Male/α1}	0.16 (32)	
Effect size of male on maximal antibody effect	$eta_{Male/\epsilon A}$	-0.34 (24)	
Error model			
Viral load (log ₁₀ copies.mL ⁻¹)	σ_V	0.80 (2)	
Spike antibodies (log ₁₀ IU.mL ⁻¹)	$\sigma_{\mathcal{A}}$	0.16 (3)	
Transition proportions (%)	σ_P	18 (2)	

Ellipses (...) indicate parameter not estimated

Abbreviations: IIV, interindividual variability; RSE, relative standard error

remdesivir [21] and nirmatrelvir/ritonavir [22], which act on viral replication only via direct inhibition, and may suggest a role for drug combination, as found in experimental models [23, 24]. Our analysis elucidated molnupiravir dual antiviral action: while direct viral inhibition occurred immediately upon treatment initiation, the mutagenesis-related effect built up more progressively and remained more sustained after treatment completion (Figure 5). However, our model did not identify a specific effect on the infectivity of viral particles [25–28]. According to our model, viral infectivity would be nonspecifically inhibited via the reduction of overall viral replication. Thus, molnupiravir would shorten viral infectiousness, not highly by preventing the formation of infectious particles, but primarily via an inhibition of viral production.

Mathematically, a drug acting purely on infectious virions would not be expected to produce a major effect on viral dynamics if administered after viral peak [29], which is the case here. Indeed, in the viral declining phase, most virus originates from cells that are already infected, and the number of new cell infections diminishes rapidly. In contrast, a drug reducing viral production would have a much stronger effect on viral load, as it would immediately

reduce the average production from infected cells. Accordingly, reproducing a sensible effect of molnupiravir on viral load requires an assumption that molnupiravir almost fully suppresses the production of infectious particles (Supplementary Table 2). This may explain why clinical trial simulation models assuming molnupiravir action only on infectious particles have estimated much higher in vivo potency of molnupiravir than estimated in vitro [30]. Here, in all scenarios, a model assuming molnupiravir action on viral production fitted the data better than assuming an effect on infectivity. We nonetheless performed a sensitivity analysis using a model where molnupiravir would act exclusively on reducing the proportion of infectious virus, with no effect on viral replication (Supplementary Table 6, Supplementary Figure 5). While showing a much larger mutation-independent antiviral effect (>90%), the model still predicted 10 days as the optimal treatment duration, as found for nirmatrelvir/ritonavir [2, 7, 31-33]. We also examined whether treatment duration could be influenced by the timing of treatment initiation. Using molnupiravir as a postexposure prophylaxis would require even longer treatment duration and suggests that 14-day administration could be relevant.

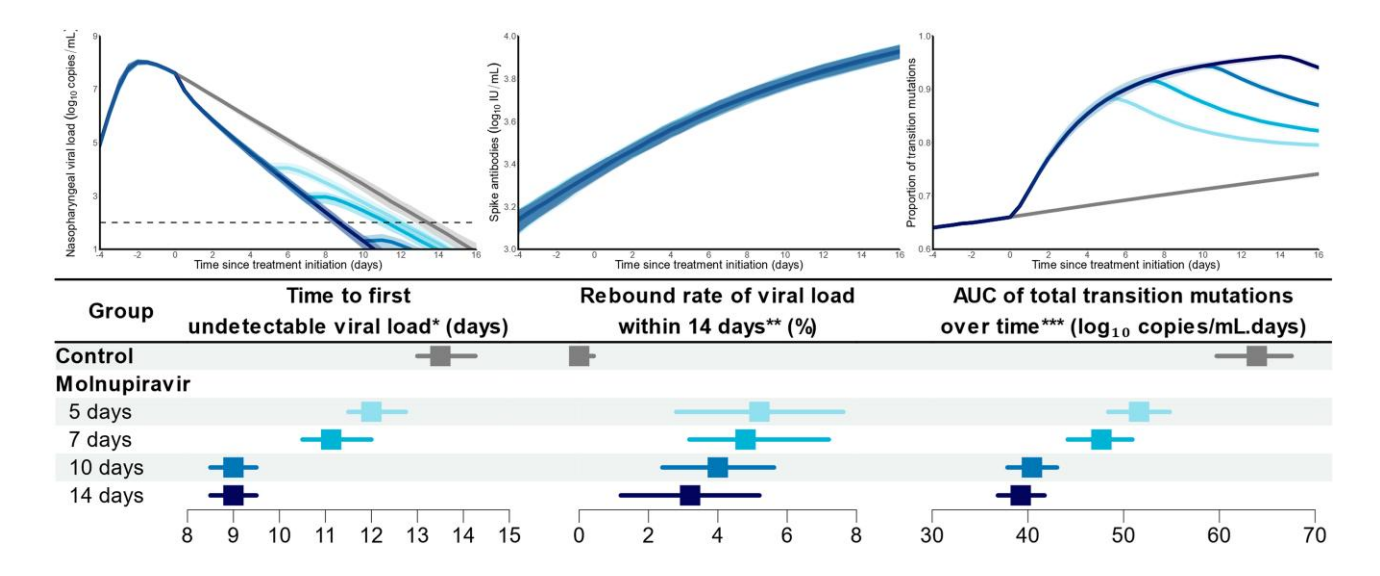


Figure 4. Predicted impact of treatment duration on viral load, spike antibodies, and proportion of transition mutations. Horizontal dashed line, limit of quantification (2.0 log₁₀ copies/mL). *Time since treatment initiation. **Time after treatment completion. ***Calculated from treatment initiation to sustained negative result on polymerase chain reaction. Results are displayed as the median profile/value and its 90% CI for 100 replicates of 250 individuals. Abbreviation: AUC, area under the curve.

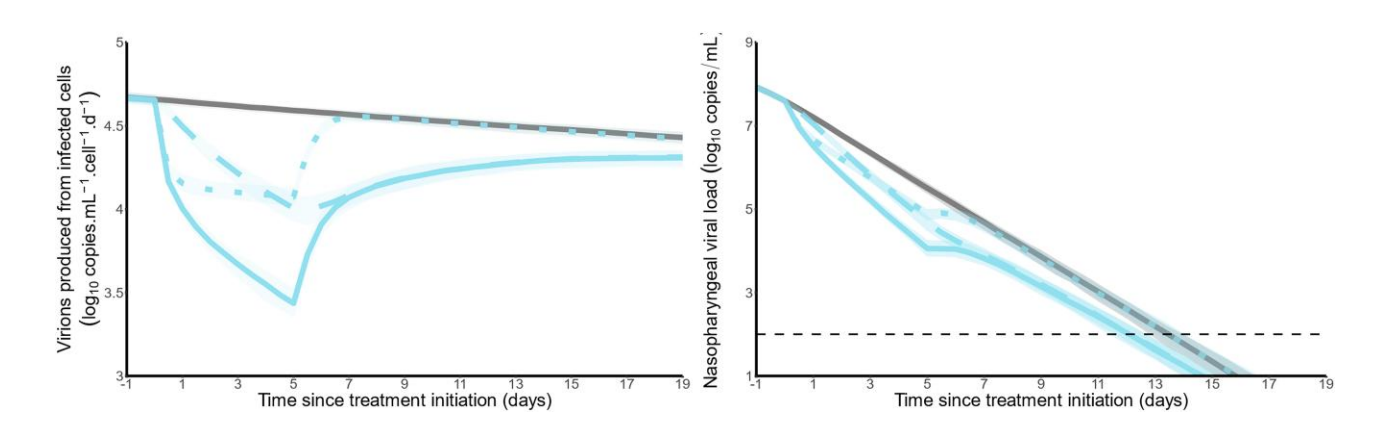


Figure 5. Molnupiravir inhibits RNA viral production via 2 mechanisms of action. Left, viral production from infected cells predicted by the model; right, impact on viral load; solid gray, control; dotted cyan, molnupiravir direct viral inhibition ($E_{M \to l}$); dashed cyan, molnupiravir viral inhibition via transition mutation only ($E_{M \to l}$); solid cyan, combined effect; horizontal dashed line, limit of quantification (2.0 log₁₀ copies/mL). Results are displayed as the median profile/value and its 90% CI for 100 replicates of 250 individuals.

Consistent with previous works [13, 31, 32, 34], our model identified the role of an interferon response—specifically, that it leads to a compartment of infection-refractory cells—thereby reinforcing the importance of innate immunity to characterize SARS-CoV-2 viral dynamics. The model also included an adaptive immune response, leading to a faster clearance of infected cells over time. Nevertheless, the model still overlooks complex mechanisms that could modify our understanding of molnupiravir's mechanism of action. First, given that the model assumes that the upper respiratory tract is one perfectly mixed environment, it does not include potential spatial and compartmentalization effects. Also, we assumed constant antibody neutralizing activity over time, which neglects the possibility that

infection-induced antibodies may have different neutralizing activity from baseline counterparts resulting from former vaccination. Another important assumption of our model involves molnupiravir pharmacokinetics with an exponential growth and decline. This might oversimplify the complex and highly variable pharmacokinetics/pharmacodynamics of molnupiravir, including its metabolism to N4-hydroxycytidine [35, 36].

It is important to underline that our model prediction about a molnupiravir-induced decrease in viral infectiousness cannot be used to discuss how the drug affect mutant formation and transmission. Indeed, without data on observed viral fitness, we did not integrate any effect of selection pressure in the model. Therefore, our model cannot predict whether

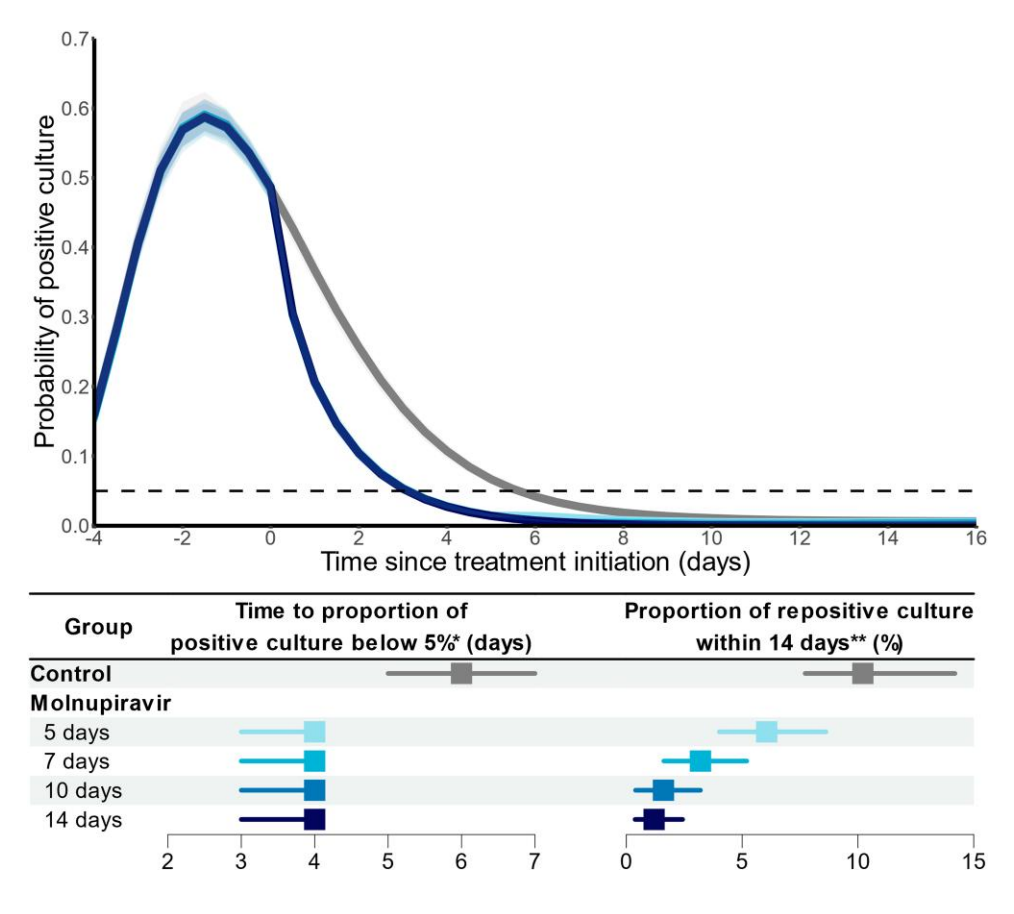


Figure 6. Predicted probability of positive culture result during treatment with molnupiravir. Horizontal dashed line, 5% threshold. *Time since treatment initiation. **Time since treatment completion. Results are displayed as the median profile/value and its 90% CI for 100 replicates of 250 individuals, assuming once-daily sampling.

molnupiravir increases the risk of generating viable highly mutant viruses. In that context, extending treatment duration of molnupiravir potentially risks generating more transmissible mutants, as SARS-CoV-2 remained culturable up to 9 days after molnupiravir cessation in 5% of treated participants [7]. Likewise, our model does not integrate the potential impact of viral rebound on symptom resolution or post–COVID-19 conditions. While our models support the use of longer courses of molnupiravir, clinical trials are therefore warranted to assess the benefit-risk of this strategy at the individual and population levels.

CONCLUSION

Our model suggests that molnupiravir achieves high-level efficacy in inhibiting viral replication. Longer administration of molnupiravir may reduce rebound rates and improve time to viral clearance.

Supplementary Data

Supplementary materials are available at *The Journal of Infectious Diseases* online (http://jid.oxfordjournals.org/). Supplementary materials consist of data provided by the author

that are published to benefit the reader. The posted materials are not copyedited. The contents of all supplementary data are the sole responsibility of the authors. Questions or messages regarding errors should be addressed to the author.

Notes

Acknowledgments. We thank all participants in the PANORAMIC virology substudy and the PANORAMIC Trial Collaborative Group.

PANORAMIC Trial Collaborative Group. Haroon Ahmed, Tanveer Ahmed, Damien Allcock, Monique Andersson, Sarah Barrett, Clare Bateman, Adrian Beltran-Martinez, Oluseye E. Benedict, Magdalena Benysek, Nicholas S. Berry, Nigel Bird, Laura Brennan, Gerard Burns, Daniel Butler, Mike Butler, Andrew Carson-Stevens, Jem Chalk, Zelda Cheng, Maria Coates, Lucy Cureton, Ruth Danson, Jennifer C. Davies, Nigel de Kare-Silver, Michelle A. Detry, Devesh Dhasmana, Jon Dickson, Melissa Dobson, Jienchi Dorward, Sarah Dowsell, Serge Engamba, Philip Evans, Stacey Fisher, Mark Fitzgerald, Robin Fox, Nick Francis, Eve Frost, Ushma Galal, Richard Gaunt, Oghenekome Gbinigie, Sarit Ghosh, Ishtiaq Gilkar, Anna Goodman, Steve Granier, Radhika Gulati, Elizabeth Hadley, Nigel D. Hart, Gail Hayward,

Richard Hobbs, Jane Holmes, Kerenza Hood, Aleksandra Howell, Iqbal Hussain, Simon Hutchinson, Marie Imlach, Greg Irving, Nicholas Jacobsen, Bhautesh Jani, James Kennard, Umar Khan, Saye Khoo, Kyle Knox, Christopher Krasucki, Layla Lavallee, Tom Law, Rem Lee, Nicola Lester, David Lewis, Mark Lown, James Lunn, Claire I. Mackintosh, Tracie-Ann Madden, Joe Marion, Mehul Mathukia, Micheal McKenna, Patrick Moore, Sam Mort, Seb Morton, Daniel Murphy, Lazaro Mwandigha, Rhiannon Nally, Chinonso Ndukauba, Jonathan S. Nguyen-Van-Tam, Emma Ogburn, Olufunto Ogundapo, Henry Okeke, Alice Packham, Amit Patel, Kavil Patel, Mahendra G. Patel, Ruth Penfold, Stavros Petrou, May Ee Png, Satveer Poonian, Olajide Popoola, Alexander Pora, Rishabh Prasad, Vibhore Prasad, Najib M. Rahman, Ivy Raymundo-Wood, Omair Razzaq, Duncan B. Richards, Scot Richardson, Simon Royal, Heather Rutter, Afsana Safa, Christina T. Saunders, Benjamin R. Saville, Satash Sehdev, Tamsin Sevenoaks, Aadil Sheikh, Vanessa Short, Baljinder S. Sidhu, Ivor Singh, Yusuf Soni, Nicholas P. B. Thomas, Andrew Ustianowski, Oliver Van Hecke, Pete Wilson, David Wingfield, Michael Wong, Nick Wooding, Sharon Woods, and Joanna Yong.

PANORAMIC Virology Group. Zaheer M. Afzal, Julie Allen, Fiona B. Ashford, Nadua Bayzid, Julianne Brown, Laura Buggiotti, Doug Burns, Samuel Ellis, Beena Emmanuel, Jose Afonso Guerra-Assuncao, Elizabeth Hadley, Jim Hatcher, Amy I. Jacobs, Emily Kirkpatrick, Luz M. Martin-Bernal, Tim McHugh, Charles Miller, Mercy Okechukwu, Alex G. Richter, Sunando Roy, Adrian Shields, Chris Thalasselis, Mia Tomlinson, Charlotte A. Williams, Rachel Williams, Maximillian Woodall, and Francis Yongblah.

Author contributions. Study design: J. F. S., D. M. L., and J. Breuer conceived and designed the virology substudy of the PANORAMIC study. B. T. N., J. Bertrand, J. F. S., and J. G. conceived and designed the modeling study. Data gathering/collection: PANORAMIC group. Data analysis and interpretation: B. T. N., J. Bertrand, J. G., A. A. A., S. Z., and J. F. S. Data management: S. Z. and J. F. S. Manuscript writing: B. T. N., J. Bertrand, J. F. S., and J. G. Manuscript review: All authors.

Disclaimer. The funders had no role in designing the study. *Financial support.* This work was supported by the Bill & Melinda Gates Foundation (INV-017335); the UK National Institute for Health and Care Research (NIHR135366); and the UK Medical Research Council (MR/X004724/1).

Potential conflicts of interest. J. F. S. has participated on a data safety monitoring board for GlaxoSmithKline (Sotrovimab) with fees paid to his institution. D. M. L. has received grants or contracts from LifeArc, the UK Medical Research Council, Bristol Myers Squibb, GlaxoSmithKline, the British Society for Antimicrobial Chemotherapy, and Blood Cancer UK; personal fees or honoraria from

Biotest UK, Gilead, and Merck; consulting fees from GlaxoSmithKline (paid to the institution); and conference support from Octapharma. J. Breuer has received consulting fees from GlaxoSmithKline (paid to her institution). All other authors report no potential conflicts.

All authors have submitted the ICMJE Form for Disclosure of Potential Conflicts of Interest. Conflicts that the editors consider relevant to the content of the manuscript have been disclosed.

References

- Bytyci J, Ying Y, Lee LYW. Immunocompromised individuals are at increased risk of COVID-19 breakthrough infection, hospitalization, and death in the post-vaccination era: a systematic review. Immun Inflamm Dis 2024; 12:e1259.
- 2. Butler CC, Hobbs FDR, Gbinigie OA, et al. Molnupiravir plus usual care versus usual care alone as early treatment for adults with COVID-19 at increased risk of adverse outcomes (PANORAMIC): an open-label, platform-adaptive randomised controlled trial. Lancet 2023; 401:281–93.
- 3. Harris V, Holmes J, Gbinigie-Thompson O, et al. Health outcomes 3 months and 6 months after molnupiravir treatment for COVID-19 for people at higher risk in the community (PANORAMIC): a randomised controlled trial. Lancet Infect Dis 2025; 25:68–79.
- Guan Y, Puenpatom A, Johnson MG, et al. Impact of molnupiravir treatment on patient-reported COVID-19 symptoms in the phase 3 MOVe-OUT trial: a randomized, placebo-controlled trial. Clin Infect Dis 2023; 77:1521–30.
- Schilling WHK, Jittamala P, Watson JA, et al. Antiviral efficacy of molnupiravir versus ritonavir-boosted nirmatrelvir in patients with early symptomatic COVID-19 (PLATCOV): an open-label, phase 2, randomised, controlled, adaptive trial. Lancet Infect Dis 2024; 24:36–45.
- Fischer WA, Eron JJ, Holman W, et al. A phase 2a clinical trial of molnupiravir in patients with COVID-19 shows accelerated SARS-CoV-2 RNA clearance and elimination of infectious virus. Sci Transl Med 2022; 14:eabl7430.
- Standing JF, Buggiotti L, Guerra-Assuncao JA, et al.Randomized controlled trial of molnupiravir SARS-CoV-2 viral and antibody response in at-risk adult outpatients. Nat Commun 2024; 15:1652.
- 8. Markov PV, Ghafari M, Beer M, et al. The evolution of SARS-CoV-2. Nat Rev Microbiol **2023**; 21:361–79.
- European Medicines Agency. Withdrawal assessment report for Lagevrio. 2023. https://www.ema.europa.eu/en/medicines/human/EPAR/lagevrio. Accessed 24 April 2024.
- Parienti JJ, de Grooth HJ. Clinical relevance of nasopharyngeal SARS-CoV-2 viral load reduction in outpatients with COVID-19. J Antimicrob Chemother 2022; 77: 2038-9.

- 11. Gonçalves A, Mentré F, Lemenuel-Diot A, Guedj J. Model averaging in viral dynamic models. AAPS J **2020**; 22:48.
- 12. Guedj J, Dahari H, Shudo E, Smith P, Perelson AS. Hepatitis C viral kinetics with the nucleoside polymerase inhibitor mericitabine (RG7128). Hepatology **2012**; 55: 1030–7.
- 13. Ke R, Martinez PP, Smith RL, et al. Daily longitudinal sampling of SARS-CoV-2 infection reveals substantial heterogeneity in infectiousness. Nat Microbiol **2022**; 7: 640–52.
- 14. Néant N, Lingas G, Le Hingrat Q, et al. Modeling SARS-CoV-2 viral kinetics and association with mortality in hospitalized patients from the French COVID cohort. Proc Natl Acad Sci U S A 2021; 118:e2017962118.
- 15. Galmiche S, Cortier T, Charmet T, et al. SARS-CoV-2 incubation period across variants of concern, individual factors, and circumstances of infection in France: a case series analysis from the ComCor study. Lancet Microbe 2023; 4: e409–17.
- Wu Y, Kang L, Guo Z, Liu J, Liu M, Liang W. Incubation period of COVID-19 caused by unique SARS-CoV-2 strains: a systematic review and meta-analysis. JAMA Netw Open 2022; 5:e2228008.
- 17. Painter WP, Holman W, Bush JA, et al. Human safety, tolerability, and pharmacokinetics of molnupiravir, a novel broad-spectrum oral antiviral agent with activity against SARS-CoV-2. Antimicrob Agents Chemother **2021**; 65: e02428-20.
- Ayral G, Si Abdallah J-F, Magnard C, Chauvin J. A novel method based on unbiased correlations tests for covariate selection in nonlinear mixed effects models: the COSSAC approach. CPT Pharmacometrics Syst Pharmacol 2021; 10:318–29.
- 19. Sheahan TP, Sims AC, Zhou S, et al. An orally bioavailable broad-spectrum antiviral inhibits SARS-CoV-2 in human airway epithelial cell cultures and multiple coronaviruses in mice. Sci Transl Med **2020**; 12:eabb5883.
- Gordon CJ, Tchesnokov EP, Schinazi RF, Götte M. Molnupiravir promotes SARS-CoV-2 mutagenesis via the RNA template. J Biol Chem 2021; 297:100770.
- 21. Kabinger F, Stiller C, Schmitzová J, et al. Mechanism of molnupiravir-induced SARS-CoV-2 mutagenesis. Nat Struct Mol Biol **2021**; 28:740–6.
- 22. Cox RM, Lieber CM, Wolf JD, et al. Comparing molnupir-avir and nirmatrelvir/ritonavir efficacy and the effects on SARS-CoV-2 transmission in animal models. Nat Commun 2023; 14:4731.
- Jeong JH, Chokkakula S, Min SC, et al. Combination therapy with nirmatrelvir and molnupiravir improves the survival of SARS-CoV-2 infected mice. Antiviral Res 2022; 208:105430.

- 24. Abdelnabi R, Maes P, de Jonghe S, Weynand B, Neyts J. Combination of the parent analogue of remdesivir (GS-441524) and molnupiravir results in a markedly potent antiviral effect in SARS-CoV-2 infected Syrian hamsters. Front Pharmacol **2022**; 13:1072202.
- Sanderson T, Hisner R, Donovan-Banfield I, et al. A molnupiravir-associated mutational signature in global SARS-CoV-2 genomes. Nature 2023; 623:594–600.
- 26. Urakova N, Kuznetsova V, Crossman DK, et al. β -D- N^4 -Hydroxycytidine is a potent anti-alphavirus compound that induces a high level of mutations in the viral genome. J Virol **2018**; 92:e01965-17.
- 27. Tian L, Pang Z, Li M, et al. Molnupiravir and its antiviral activity against COVID-19. Front Immunol **2022**; 13: 855496.
- 28. Malone B, Campbell EA. Molnupiravir: coding for catastrophe. Nat Struct Mol Biol **2021**; 28:706–8.
- Gonçalves A, Bertrand J, Ke R, et al. Timing of antiviral treatment initiation is critical to reduce SARS-CoV-2 viral load.
 CPT Pharmacometrics Syst Pharmacol 2020; 9:509–14.
- 30. Esmaeili S, Owens K, Standing JF, et al. Molnupiravir clinical trial simulation suggests that polymerase chain reaction underestimates antiviral potency against SARS-CoV-2. medRxiv. Preprint posted online 6 January 2025. https://doi.org/10.1101/2024.11.21.24317726
- 31. Owens K, Esmaeili-Wellman S, Schiffer JT. Heterogeneous SARS-CoV-2 kinetics due to variable timing and intensity of immune responses. JCI Insight **2024**; 9. https://doi.org/10.1172/jci.insight.176286
- 32. Esmaeili S, Owens K, Wagoner J, Polyak SJ, White JM, Schiffer JT. A unifying model to explain frequent SARS-CoV-2 rebound after nirmatrelvir treatment and limited prophylactic efficacy. Nat Commun 2024; 15:5478.
- Donovan-Banfield I, Penrice-Randal R, Goldswain H, et al. Characterisation of SARS-CoV-2 genomic variation in response to molnupiravir treatment in the AGILE phase IIa clinical trial. Nat Commun 2022; 13:7284.
- Perelson AS, Ribeiro RM, Phan T. An explanation for SARS-CoV-2 rebound after Paxlovid treatment. medRxiv. Preprint posted online 1 June 2023. https://doi. org/10.1101/2023.05.30.23290747
- 35. Gouda AS, Marzouk HM, Rezk MR, et al. A validated LC-MS/MS method for determination of antiviral prodrug molnupiravir in human plasma and its application for a pharmacokinetic modeling study in healthy Egyptian volunteers. J Chromatogr B Analyt Technol Biomed Life Sci 2022; 1206:123363.
- European Medicines Agency. Assessment report for use of molnupiravir for the treatment of COVID-19. 2022. https://www.ema.europa.eu/en/medicines/human/EPAR/ lagevrio. Accessed 10 April 2024.